Mössbauer Studies

Mineralogy and Composition of Lunar Fines and Selected Rocks

Abstract. *Mineralogical descriptions and both wet chemical analyses and microprobe analyses are given of the glasses and crystalline components of the lunar fines and of the minerals in microgabbros (samples 10050 and 10047). The principal minerals described are various clinopyroxenes, plagioclase, olivine, low cristobalite, low tridymite, ilmenite, iron-nickel, iron, schreibersite, cohenite, troilite, and a new CaFe pyroxenoid. Descriptions are given of small craters produced by hypervelocity particle impact on glass and iron-nickel fragments in the fines. The rounding of grains in the fines and of surface rocks is attributed to mechanical abrasion and not to cratering.*

Approximately half of the lunar fines (<1 mm) consist of particles below 37 μm in size. Wet chemical analyses of the bulk fines, of the <37-μm fraction, of an abundant scoriaceous glass component, and of the microbreccia rock show almost identical compositions (Table 1, analyses 1 to 4). Analyses of the microgabbro and vesicular basalt (Table 1, analyses 5 and 6) show somewhat higher FeO and TiO_2 and less Al_2O_3, with a higher K_2O content in the basalt. These differences probably arise because the two rock analyses are not representative of the rock suite from which the fines, the glass, and the microbreccia were derived.

Glasses in the fines occur as spheroids and other rounded forms and as angular or abraded fragments, which vary from colorless ($d \leq 2.6$ g/cm^3; n, 1.46 to 1.60), pale yellow, yellow-brown, tan, and green shades ($d \sim 2.7$ to 2.8, $n \sim 1.59$ to 1.65), dark brown and reddish brown ($d \sim 2.9$ to 3.1, $n \sim 1.65$ to 1.75) to almost opaque ($d \sim 3.1$ to 3.3, $n \sim 1.75$). A dark brown scoriaceous glass (Table 1, analysis 3) shows color banding and contains minute spherical iron inclusions and unfused inclusions of clinopyroxene, ilmenite, plagioclase, and lithic fragments. Plagioclase glasses (61 to 94 percent anorthite) and compositions between anorthite and the scoriaceous glass are less abundant. Figure 1 shows glass compositions that range from plagioclase to glasses higher in FeO and TiO_2 than the scoriaceous material. They can be formed by varying admixtures of plagioclase, clinopyroxene, and ilmenite.

The crystalline phases in the fines

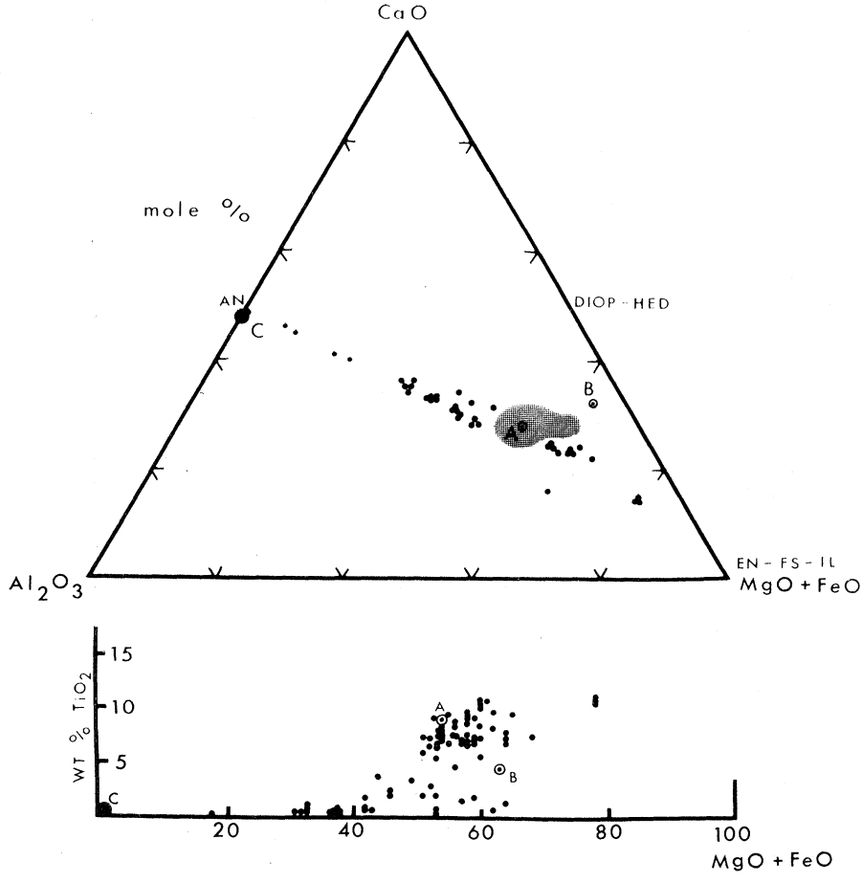

Fig. 1. (Top) Electron probe analyses (J. C. Drake, analyst) of glasses in lunar fines in terms of molecular percentages of CaO, Al_2O_3, and (MgO + FeO). Each dot represents the analysis of a single glass spherule, dumbbell, or angular fragment. The shaded area represents 48 analyses. Point A is a plot of the scoriaceous glass analysis in Table 1 (analysis 3) and point B is a plot of the two clinopyroxene analyses in Table 2 (analyses 1 and 2). Point C is an average of 15 plagioclase glasses (from 61 to 94 percent anorthite). In general, the density of the glasses increases from left to right, from $d \leq 2.6$ to $d \sim 3.25$. Abbreviations are An (anorthite), Diop (diopside), Hed (hedenbergite), En (enstatite), Fs (ferrosilite), Il (ilmenite). (Bottom) Percentage by weight of TiO_2 in the glasses as a function of (MgO + FeO).

Table 1. Wet chemical analyses of bulk fines (< 1 mm), glass in fines, and rock fragments in coarse fines (1 cm to 1 mm).

Component	Average fines*	Fine fines†	Scoriaceous glass‡	Microbreccia§	Fine-grained gabbro‖	Vesicular basalt¶
	No. 1	No. 2	No. 3	No. 4	No. 5	No. 6
SiO_2	41.77	41.81	41.84	41.69	41.65	40.60
TiO_2	7.42	7.20	7.09	7.35	8.79	11.28
Al_2O_3	13.68	14.64	14.00	13.52	11.00	8.05
Cr_2O_3	0.36	0.31	0.30	0.36	0.34	0.33
FeO (total)	15.98	15.21	15.78	16.05	18.20	20.09
MnO	0.23	0.20	0.23	0.23	0.25	0.24
MgO	8.38	7.55	8.18	8.40	7.80	7.90
CaO	11.68	12.59	12.03	11.76	11.22	10.57
Na_2O	0.41	0.43	0.40	0.42	0.41	0.44
K_2O	0.13	0.14	0.14	0.14	0.12	0.24
P_2O_5	0.12	0.1	0.1	0.12	0.12	0.15
NiO	~0.01	~0.01	~0.01	0.01		
ZrO_2	0.05	0.05	0.05	~0.06	~0.1	~0.1
S	0.1	0.1	0.1	~0.1	~0.1	~0.2
$-S=O$	−0.05	−0.05	−0.05	−0.05	−0.05	−0.1
Total	100.20	100.24	100.15	100.16	100.05	100.09

* Particle size < 1 mm; sample weight, 1.16 g. † Particle size < 37 μm; sample weight. 1.01 g. ‡ Mixture of approximately 60 percent dark brown glass and 40 percent enclosed or adhering clinopyroxene, plagioclase, and ilmenite; sample weight. 0.52 g. § Sample weight, 1.05 g. || Approximately 50 percent tan clinopyroxene, 35 percent plagioclase, 15 percent ilmenite, and rare olivine and cristobalite; trace of troilite with iron blebs; sample weight, 1.07 g. ¶ Approximately 50 percent tan clinopyroxene, 30 percent plagioclase, 20 percent ilmenite, and traces of troilite with iron blebs; sample weight, 1.06 g.

Table 2. Wet chemical analyses of clinopyroxene (Nos. 1 and 2), plagioclase (Nos. 3 and 4), and ilmenite (No. 5) in lunar fines and fine-grained gabbro. Clinopyroxene No. 1 and plagioclase No. 3 from lunar fines; clinopyroxene No. 2, plagioclase No. 4, and ilmenite No. 5 from fine-grained gabbro (10050,37).

Component	Clinopyroxene		Plagioclase		Ilmenite
	No. 1*	No. 2*	No. 3†	No. 4‡	No. 5§
SiO_2	48.2	49.2	45.1	46.3	
TiO_2 (total)	3.38	2.58	0.05	0.05	52.6
Al_2O_3	4.65	3.55	35.1	34.0	
Cr_2O_3 (total)	0.53	0.46	0.01	0.01	0.51
FeO (total)	12.45	12.62	0.42	0.99	45.3
MnO	0.23	0.24	0.03	0.03	0.37
MgO	15.1	16.0	0.3	0.3	0.83
CaO	15.25	15.20	18.0	17.1	
Na_2O	0.12	0.10	0.85	1.05	
K_2O			0.07	0.09	
ZrO_2	~0.02	~0.02			~0.3
Total	99.93	99.97	99.9	99.9	99.9
	Number of ions on the basis				
	Of 6 oxygens		*Of 8 oxygens*		*Of 3 oxygens*
Si	1.808	1.844	2.082	2.135	
Al	0.192 (2.00)	0.156 (2.00)	1.910 (3.99)	1.848 (3.98)	
Al	0.014	0.001			
Ti	0.095	0.073	0.002	0.002	0.994
Cr	0.016	0.013			0.010
Fe	0.391	0.395	0.016	0.038	0.952
Mn	0.007 (1.99)	0.008 (2.00)	0.001 (1.01)	0.001 (1.00)	0.008 (0.99)
Mg	0.844	0.893	0.020	0.020	0.031
Ca	0.613	0.610	0.890	0.845	
Na	0.009	0.007	0.076	0.094	
K			0.004	0.005	
Zr					0.002
Mg	45.7	47.0	An 91.7	An 89.5	
Fe	21.1	20.8	Ab 7.8	Ab 9.9	
Ca	33.2	32.1	Or 0.4	Or 0.5	

* Both samples contain approximately 0.5 percent (by volume) ilmenite as inclusions. This ilmenite was not deducted from the analysis. Weight: sample 1, 0.36 g; sample 2, 0.45 g. † This sample (weight, 0.27 g) contained 4 percent by weight impurity (0.35 percent ilmenite and 3.65 percent clinopyroxene). These impurities were substracted and the analysis was recalculated to 100 percent. TiO_2 and MgO values were obtained by electron probe. ‡ The sample (weight, 0.36 g) contained 2.3 percent by weight impurity (0.46 percent ilmenite and 1.84 percent clinopyroxene). These impurities were subtracted, and the analysis was recalculated to 100 percent. TiO_2 and MgO values were obtained by electron probe. § The sample (weight, 0.22 g) contained 8.5 percent by weight adhering clinopyroxene and plagioclase. The analysis was recalculated to 100 percent after subtraction of these phases. Electron probe analyses showed absence of Al.

include (in decreasing abundance) clinopyroxenes, plagioclase, ilmenite, olivine, tridymite, cristobalite, iron-nickel, iron, troilite, schreibersite, and cohenite. The pyroxenes are highly inhomogeneous and vary from augite, in part with exsolved pigeonite, to subcalcic augite, pigeonite, ferroaugite, and titanaugite. A wet chemical analysis of a bulk, average sample of the pyroxene is given (Table 2, analysis 1). Figure 2 shows probe analyses of clinopyroxene grains. The titanaugite in Fig. 2 represents a brown, almost opaque type containing ilmenite inclusions. A wet analysis of bulk anorthite from the fines corresponds to 92 percent anorthite (Table 2, analysis 3). The total variation in anorthite content, determined by probe analyses of individual grains, ranges from 90 to 98 percent anorthite. Ilmenite is the main accessory mineral. Olivine is yellowish green and transparent, and varies from approximately 61 to 76 percent forsterite. Low cristobalite occurs rarely as microgranular grains with n 1.486 and birefringence ~0.002. Low tridymite occurs sparingly as grains with irregular extinction and inversion twinning. The indices of refraction (α 1.470, β 1.472, γ 1.476) are relatively low. Isotropic silica glass (n 1.462), probably derived from tridymite, was tentatively identified. Wavy intergrowths of colorless glasses with $n \sim 1.462$ and colored, high index glasses were observed. Iron-nickel (~3 to 14 percent Ni, mostly 6 to 7 percent Ni) occurs rarely as spheroidal and discoidal bodies, as cubo-octahedrons, and as fragments of meteoritic iron. Iron (<0.5 percent Ni) occurs as tiny spheres, cubical crystals, and thin films in glass, and as grains intergrown with plagioclase and pyroxene. The iron-nickel is intergrown with schreibersite, cohenite, and troilite.

Microgabbro 10050,37 was studied in detail, and wet analyses of the clinopyroxene, anorthite, and ilmenite from this sample are given in Table 2 (analyses 2, 4, and 5). Compositionally, the pyroxenes are extremely variable. Figure 2 shows the bulk pyroxene analysis and the compositional variations from augite, with pigeonite, to iron-rich pyroxenes. The outer edges of large grains, and smaller clinopyroxene grains interstitial to plagioclase, have the most Fe-rich compositions. The range in TiO_2 content of the pyroxenes is from 0.6 to 5.1 percent by weight, and Al_2O_3 ranges from 0.5 to

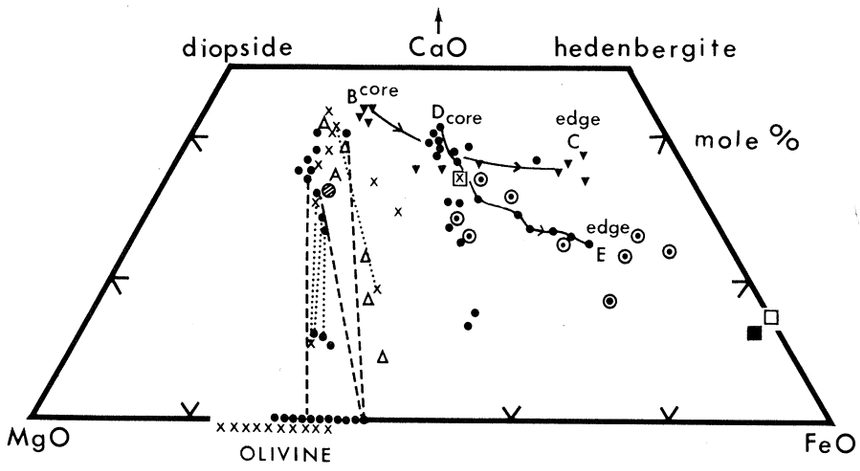

Fig. 2. Pyroxene, olivine, and pyroxenoid compositions in rocks and fines in terms of molecular percentages of CaO, MgO, and FeO. All compositions, except point *A*, are electron microprobe determinations (C. Klein and J. C. Drake, analysts). Point *A* represents the bulk analyses of the two clinopyroxenes in Table 2 (analyses 1 and 2). The symbols represent pyroxenes, olivines, and pyroxenoid in different assemblages: (solid circle) olivine and pyroxene in rock 10050,37 (fine-grained gabbro); (solid circle in ring) fine-grained, interstitial, yellowish tan pyroxene in 10050,37; (inverted solid triangle) pyroxenes in rock 10062,34 (gabbro); (open triangle) pyroxenes in rock 10045,32 (vesicular ilmenite basalt); (cross) pyroxene and olivine in fines; (cross in square) titanaugite in fines (TiO_2, 7.0 percent by weight); (solid square) yellow phase in rock 10047 similar to synthetic Ca-Fe pyroxenoid (C. W. Burnham and D. H. Lindsley, personal communication; their synthetic composition is shown by the open square). Dotted lines connect coexisting augite and pigeonite in fines and rocks. Dashed lines connect coexisting augite and olivine. Lines *B–C* and *D–E* represent probe traverses across single pyroxene grains, from core to edge (traverse length, approximately 250 μm).

6.0 percent by weight. The average plagioclase is 90 percent anorthite; the total range is from 84 to 94 percent anorthite. The anorthite probably contains some Fe in its structure. The accessory ilmenite is the main host mineral for Zr (Table 2, analysis 5). The olivines, from 58 to 70 percent forsterite, occur as rounded or bleb-like grains in clinopyroxene. Low cristobalite occurs sparingly as flattened octahedrons that are oriented microgranular inversion pseudomorphs after high cristobalite. Low tridymite occurs as inversion pseudomorphs after crystals of high tridymite, which are tabular on (0001). Both minerals show inversion twinning. Troilite, an accessory mineral, shows exsolution blebs of iron. An unidentified yellow-brown mineral containing Fe and probably Cl that decomposes under the electron beam was noted.

In microgabbro 10047 a new yellow mineral (with α 1.752, β 1.758, and δ 1.767, faintly pleochroic) consisted of CaO 6.0, FeO 47.2, MgO 0.9, MnO 1.0, Al_2O_3 0.2, TiO_2 0.5, SiO_2 45.0 percent by weight (total 100.8), corresponding to $Ca_{13}Mg_3Fe_{84}$. It has a composition similar to, and an x-ray powder pattern identical with, that of a synthetic pyroxenoid of composition $Ca_{15}Fe_{85}$ (*1*).

Impact craters produced by hypervelocity particles and ranging up to about 1 mm in diameter are common on spherules and fragments of the glass and iron-nickel in the fines. The craters have a complex morphology: in nickel-iron, a surface rim and two inner subcraters of different diameter; in glass, two subcraters, the inner with a rim of glass, a zone of granulated glass, and an outer shallow fracture crater. These impact craters are viewed as a transient event, produced while the material was in free flight in the explosion cloud of a meteorite impact in which the hypervelocity particles were themselves generated.

Well-rounded, abraded grains of glass, of plagioclase, of pyroxene, and of lithic fragments are common; they resemble terrestrial detrital sands. These features, and the rounding of large rock fragments on the lunar surface, are attributed to abrasion attending meteorite impacts. The surface material also was impacted by hypervelocity particles at the same time.

CLIFFORD FRONDEL
CORNELIS KLEIN, JR.
JUN ITO, JOHN C. DRAKE
Department of Geological Sciences,
Harvard University,
Cambridge, Massachusetts 02138

Reference and Note

1. C. W. Burnham and D. H. Lindsley, personal communication.
2. Supported by NASA contract NAS-9-8100. We thank C. W. Burnham and M. Campot for assistance.

4 January 1970

Mössbauer Spectrometry of Lunar Samples

Abstract. *Nuclear gamma resonance measurements for the nuclide ^{57}Fe in lunar material were made in transmission on lunar fines and in scattering on intact lunar rock chips. No appreciable amount of ferric iron was detected. Resonances were observed for ilmenite in all samples. Strong resonances attributed to ferrous iron in silicates, including pyroxenes and, in some samples, glasses and olivine, were also present. Metallic iron, alloyed with nickel, and troilite were also detected in the lunar fines. Differences in the spectra of various samples of lunar material and their significance are discussed.*

This paper reports on the application of Mössbauer spectrometry (*1-3*) to lunar material. Mössbauer spectrometry is appropriate for the study of solid materials that contain appreciable concentrations of elements that exhibit nuclear gamma resonance. These elements include iron, one of the major elements in the material returned to earth by Apollo 11 (*4*), and which was detected in each remote chemical analysis at Surveyor sites on the moon (*5*).

This technique has proved especially useful for the identification and characterization of iron-bearing minerals and mineraloids, determination of the phase distribution of the iron, and determination of the oxidation state of the iron in the sample. It involves the measurement of nuclear hyperfine spectra of iron atoms in the lunar material by determination of the energy spectrum of the resonance absorption of nuclear gamma radiation transmitted through